

Published in final edited form as:

Pediatr Res. 2016 August ; 80(2): 299–305. doi:10.1038/pr.2016.72.

Metabolites involved in Glycolysis and Amino Acid Metabolism are Altered in Short Children Born Small for Gestational Age

Philip G Murray¹, Imogen Butcher¹, Warwick B Dunn^{2,3,4}, Adam Stevens¹, Reena Perchard¹, Daniel Hanson¹, Andrew Whatmore¹, Melissa Westwood⁵, and Peter E Clayton¹

¹Centres for Paediatrics and Child Health, Institute of Human Development, University of Manchester and Central Manchester University Hospitals NHS Foundation Trust, Manchester Academic Health Sciences Centre, Royal Manchester Children's Hospital, Oxford Road, Manchester, M13 9WL, UK.

²Centre for Advanced Discovery & Experimental Therapeutics (CADET), Institute of Human Development, University of Manchester and Central Manchester University Hospitals NHS Foundation Trust, Manchester Academic Health Sciences Centre, Nowgen Centre, Grafton Street, Manchester, M13 9WU, UK.

³Manchester Centre for Integrative Systems Biology, School of Chemistry, University of Manchester, Princess Street, Manchester, M1 7DN, UK

⁴School of Biosciences, University of Birmingham, Edgbaston, Birmingham, B15 2TT, UK

⁵Maternal and Fetal Health Research Centre, Institute of Human Development, University of Manchester and Central Manchester University Hospitals NHS Foundation Trust, Manchester Academic Health Sciences Centre, St Mary's Hospital, Manchester, Oxford Road, Manchester, M13 9WL, UK.

Abstract

Background—Later life metabolic dysfunction is a well-recognised consequence of being born Small for Gestational Age (SGA). This study has applied metabolomics to identify whether there are changes in these pathways in pre-pubertal short SGA children and aimed to compare the intracellular and extracellular metabolome in fibroblasts derived from healthy children and SGA children with post-natal growth impairment.

Methods—Skin fibroblast cell lines were established from eight SGA children (age 1.8 -10.3 years) with failure of catch-up growth and from three healthy control children. Confluent cells were incubated in serum free media and the spent growth medium (metabolic footprint) and intracellular metabolome (metabolic fingerprint) were analysed by gas-chromatography mass spectrometry.

Users may view, print, copy, and download text and data-mine the content in such documents, for the purposes of academic research, subject always to the full Conditions of use:http://www.nature.com/authors/editorial_policies/license.html#terms

Correspondence and requests for reprints to Dr Philip Murray, 5th Floor (Research), Royal Manchester Children's Hospital Oxford Road, Manchester, M13 9WL, UK Philip.Murray@manchester.ac.uk Tel: +44 (0)161 701 7563.

Disclosure statement - PGM, WBD, MB, AW, AS, GCB and MW have nothing to declare. IB was the recipient of an unrestricted educational grant from NovoNordisk. PEC has received lecture fees from NovoNordisk.

Results—19 metabolites were significantly altered between SGA and control cell lines. The greatest fold difference (FD) was seen for alanine (fingerprint FD, SGA: control) 0.3, $p=0.01$ and footprint FD=0.19, $p=0.01$), aspartic acid (fingerprint FD=5.21, $p=0.01$) and cystine (footprint FD=1.66, $p=0.02$). Network analysis of the differentially expressed metabolites predicted inhibition of insulin and activation of ERK/AKT/PI3K signalling in SGA cells.

Conclusions—This study indicates that changes in cellular metabolism associated with both growth failure and insulin insensitivity are present in pre-pubertal short children born SGA.

Keywords

SGA; Metabolome; 3-M syndrome; CUL7; OBSL1; CCDC8

Introduction

There are approximately 700,000 children born in the UK each year¹. Using a definition of small for gestational age (SGA) as a birth weight more than 2 standard deviations below mean birth weight, there are approximately 16,000 SGA children born each year. SGA neonates can broadly be divided into those who are constitutionally small (i.e. small in comparison to population standards but normal for familial and ethnic background) and those with pathological growth impairment². Intra uterine growth restriction is a term applied to foetuses and neonates with an estimated fetal weight or birth weight/length <10th percentile due to pathological growth restriction due to adverse genetic or environmental influences³. Around 10% of children born SGA will fail to show catch-up growth over the first two years of life, leaving approximately 1600 children in the UK who remain short (height SDS < -2) at two years of age⁴. As well as growth impairment children born SGA are at increased risk of cardiovascular disease, hypertension, hyperlipidaemia and type 2 diabetes in adulthood⁵.

The causes of children being born SGA are numerous and include maternal, placental and fetal factors⁵. There are a small number of monogenic causes for a child to be born SGA and experience poor post-natal growth (e.g. 3-M syndrome, Bloom syndrome, Microcephalic Osteodysplastic dwarfism type II, IGF-IR mutations, Seckel syndrome, and Mulibrey nanism)⁶.

Metabolomics provides a number of advantages over single analyte measurement, for example, high-throughput analytical strategies and the provision of a dynamic and sensitive measure of all metabolites that contribute to the phenotype being examined⁷. In mammals metabolomics is typically applied in the discovery of novel biomarkers of disease⁸⁻¹¹, drug efficacy¹² or toxicity¹⁰, or is used to understand molecular pathophysiological mechanisms¹²⁻¹⁴. In mammalian systems; metabolites act as building blocks for larger molecules (e.g. proteins) and structures (e.g. lipids in cell walls) and they act to regulate biochemical processes (e.g. allostereism) and as signalling molecules⁷. When studying cultured mammalian cells and tissues, two separate but linked metabolomes can be studied; the intracellular metabolome (metabolic fingerprint) and the extracellular metabolome (metabolic footprint). The metabolic fingerprint allows a snapshot of cellular metabolism to be obtained while the footprint reflects the effects of metabolite uptake and secretion.

This study has used an established ex-vivo skin fibroblast cell model as previous work has shown this to be a good model for examining growth disorders¹⁵⁻¹⁷. The aim of this study was to elucidate potential novel pathophysiological mechanisms associated with 1) failure of postnatal catch-up growth in SGA children and 2) the well-recognised predisposition to metabolic morbidity and diabetes in later life in short children SGA¹⁸. While previous studies have examined serum and urine metabolomics in SGA/IUGR children¹⁹⁻²¹ by utilising a cell based model it is possible to gain deeper insight into intracellular metabolism, potentially yielding useful information on the mechanisms underlying the growth impairment and metabolic changes seen in these patients.

Results

In the metabolic fingerprint study, 93 unique chromatographic peaks (related to 38 unique and identified metabolites) were detected in the samples from both control and SGA cells. In the metabolic footprint study, 95 unique chromatographic peaks were detected in all samples studied; these related to 39 unique and identified metabolites.

Comparing the metabolome (fingerprint and footprint) of all the SGA patient cells (n=8) to controls (n=3), 29 metabolic peaks representing 8 unique and identified metabolites in the fingerprint and 11 unique and identified metabolites in the footprint were statistically significantly up- or down-regulated (Table 1). The amino acid alanine was down-regulated in the SGA cell lines in both footprint (Fold Difference (FD) =0.33) and fingerprint (FD=0.19). There were 5 amino acids up-regulated in the metabolic fingerprint of the SGA cell lines; threonine, ornithine, serine, aspartic acid and glutamic acid. The only metabolites not classified as amino acids and identified in the fingerprint were the carbohydrate fructose which was upregulated in the SGA cell lines (FD=1.8) and the Krebs cycle intermediary, citric acid, which was also up-regulated (FD=1.53). In the metabolic footprint data, the amino acids cysteine (FD=0.32) and phenylalanine (FD=0.65) were downregulated in SGA cell lines while cystine was up-regulated (FD=1.66). Pyruvic acid was up-regulated and 2-methyl-3-hydroxybutanoic acid and 3-methylpentanoic acid were down-regulated in the SGA cell lines.

Subgroup analysis comparing the 3-M syndrome and non-3-M syndrome patients both to control and to each other also identified differences in the metabolomics fingerprint and footprint (see supplemental Tables 1-3). Of the 18 metabolic peaks identified as differentially regulated between control and 3-M patients only three (inositol-1-phosphate, glutamine and 2-oxopropanoic acid) were not also identified as dysregulated in the whole group analysis. There were also 18 metabolites significantly different between the non-3-M patients and controls of which three (myo-inositol, lysine and phosphate) were not identified as being dysregulated between all patients and controls. There were 5 metabolic peaks in the fingerprint (alanine, aspartic acid, fructose, ornithine and serine) and three in the footprint (3-methylpentanoic acid, alanine and cysteine) significantly different to controls for all the patients as well as in both the subgroup analyses of 3-M and non 3-M patients. There were 21 different metabolites significantly up or down-regulated between the 3-M and non-3-M patients (Supplementary Table 3) including 9 metabolites in the footprint and 11 in the fingerprint.

Metabolic Pathway Enrichment Analysis, using MetaboAnalyst was performed by including all unique and statistically significant metabolites detected in the metabolic fingerprint and footprint samples when comparing all the SGA patient cells to controls. Five metabolic pathways showed enrichment with a false discovery rate of $q < 0.05$ (see Table 2).

An interaction network formed from the metabolites identified as differentially regulated between all SGA patient and control cell lines contained PI3K, AKT, p38 and ERK in addition to molecules in the proinsulin-insulin pathway (Figure 1). This interaction network predicts inhibition insulin activity. Biological functions associated with the differentially regulated metabolites included carbohydrate metabolism, cell-cell signalling, cell growth and cell cycle (see Figure 2).

The identification of these protein kinases in the network led us to validate their involvement by examining the activation of kinases in response to IGF-I using a phosphokinase array in the cell lines. Treatment with IGF-I led to a significant change ($p < 0.05$) in phosphorylation of 9 proteins in control cells (ERK1, ERK2, JNK1, JNK2, pan JNK, p38, RSK2, pan AKT and MSK2) and 8 proteins in the SGA cells (ERK1, JNK1, p38, RSK1, RSK2, AKT2 and MSK2) (see Figure 3). These data imply that in control but not in SGA cells IGF-I preferentially activates ERK2 and JNK2 while, in SGA but not controls, IGF-I preferentially activates RSK1. Both ERK2 and JNK are contained within the interaction network formed from the differentially regulated metabolites (Figure 1) and are linked via glutamic acid.

Discussion

The primary aim of this study was to identify metabolomic changes in fibroblasts from children with a severe SGA/growth impairment syndrome and to identify pathogenic mechanisms linking these metabolomic changes to short stature and/or early markers of metabolic disease. There are limited data available on metabolomic changes in SGA children: one study identified changes in the metabolome in media conditioned by placental explants from pregnancies complicated by SGA²². 79 metabolites were altered including aconitate, lithospermic acid, tryptophan and oxoproline. Alterations of multiple metabolites, including amino acids, lipids and myo-inositol, have been identified in the serum of piglets with intra-uterine growth restriction²³. Dessi et al²⁰ studied the urinary metabolome in intra-uterine growth restricted (IUGR) and normal weight newborns and identified differences in the concentrations of myo-inositol and creatinine (both up-regulated). An increase in myo-inositol was demonstrated in a second cohort of IUGR infants as well as in large for gestational age infants^{19,24}. The IUGR infants from the studies of Dessi *et al* used a definition of weight at birth $< 10^{\text{th}}$ centile and so may have included in the IUGR group newborns who would be classed as normal based on a definition of SGA being a weight SDS < -2 . Another study compared the metabolome from cord blood samples of SGA and AGA infants and identified increases in the amino acids proline, valine, isoleucine, glutamate, phenylalanine and tryptophan²⁵. Work from our own laboratory studying the serum and urine metabolome of 33 SGA children (all age > 4 years, 22 catch up and 11 non-catch up) identified significant differences in myo-inositol (in urine), decanoic acid (in serum), glutamine (in serum), uric acid (in urine) and carnitine (in urine)²¹. The most consistently identified metabolite altered in SGA/IUGR appears to be myo-inositol. With the

exception of phenylalanine the metabolites identified as being altered in SGA in this study are different to those identified in other studies, which represents the differences in examining biofluids (urine or serum) compared to the cellular metabolome.

A cell model were chosen for this study in order to allow examination of a snapshot of the intracellular metabolism as previous studies have focused on serum, urine and conditioned media (all of which provide information on longer term metabolic uptake and secretion). Fibroblasts were chosen as they have previously been shown to be a good model for studying growth disorders¹⁵⁻¹⁷ and are easy to obtain via a skin biopsy. For studying the effects of being SGA on glucose, fat or lipid metabolism it may be better to dedifferentiate the fibroblasts into induced pluripotent stem cells and then re-differentiate the stem cells into adipocytes or hepatocytes. The growth and metabolic changes seen in short children born SGA represent long term modifications to cellular processes. Studying a cultured fibroblast cell line rather than tissue avoids the possibility of local factors at the time of biopsy (e.g. trauma) influencing results.

In this study there were decreases in 2-methyl-3-hydroxybutanoic acid and 3-methylpentanoic acid which are both organic acids generated by isoleucine metabolism. Isoleucine is one of the three branched chain amino acids and increases in levels of the branched chain amino acids are linked to obesity and insulin resistance²⁶. A second observation was related to the depletion of the intracellular alanine pool either as a result of increased production of aspartic acid, glutamic acid and ornithine or as a result of reduced conversion of pyruvate to alanine via alanine transferase. Alanine was present at a 4 fold lower concentration in SGA subjects while aspartic acid was present at a 4 fold higher concentration in the metabolic fingerprint and pyruvate at 1.4 fold higher concentration. Ornithine and glutamic acid, both products of alanine catabolism, were present at 1.4 fold higher concentrations in SGA subjects in the metabolic fingerprint. Thus there is evidence for both reduced production and increased catabolism of alanine. Abnormalities in alanine and branched chain amino acids have been linked to cardiovascular disease as a rise in these metabolites is found in populations in China where there are increased rates of cardiovascular disease and obesity²⁷. Alterations in the levels of alanine, threonine and the branched chain amino acids have also been found in infants born with weight of less than 1500g (this study included premature infants, hence not all infants will have been SGA)²⁸.

Biological network analysis of the footprint and fingerprint metabolomic data obtained in this study identified a network involving insulin, PI3K, ERK and AKT. The biological functions significantly associated with the differentially regulated metabolites included cell growth, cell cycle and carbohydrate metabolism. PI3K, ERK and AKT are involved in the signal transduction pathways of both insulin and IGF-I receptors. Alterations signal transduction of IGF-I and insulin is a plausible mechanism to cause both the growth and metabolic effects seen in SGA children. Increased activity within growth related pathways has previously been associated with short stature disorders such as Noonan syndrome²⁹ while inhibition of insulin signalling is seen in Donohue syndrome, also associated with growth restriction³⁰. This study therefore strengthens the suggestion that the cellular metabolic pathways involved in glucose regulation and growth are altered in SGA children. The phospho-kinase array identified differences between the control and SGA cell lines in

the activation of growth related signalling pathways and these were represented in the network analysis (ERK, JNK2 and RSK2).

This study has identified multiple metabolomic changes in fibroblasts from SGA children. Horgan et al³¹ identified a serum metabolomic profile in early pregnancy which was predictive of the child being born SGA. Further work is required to determine if any of these metabolomic changes can be used either in utero or during the first few months of life to predict subsequent growth and metabolic health in SGA children. The limitations of the study include the small number of subjects and the use of GC-MS only. The application of liquid-chromatography-mass spectrometry would increase the coverage of metabolites detected. Evidence is presented for changes in growth and glucose metabolism pathways in skin fibroblast cell lines derived from SGA children. Further extensive studies are required to identify whether changes in the metabolome may correlate with growth phenotype, for instance differentiating those SGA children who are destined either to experience inadequate catch up growth, full catch-up or even excessive weight gain. In particular future studies should focus on expanding this work into the clinical arena with prospective studies in babies born SGA.

In conclusion we have identified intracellular metabolomic changes linked in network analysis to reduced insulin and IGF-I signal transduction in fibroblasts derived from short children born SGA.

Material and Methods

Patients

Patients were recruited from the regional Growth Clinic at the Royal Manchester Children's Hospital. They were eligible for inclusion where they were born small for gestational age (birth weight SDS -2 SD) and had either failure of catch up growth with height SDS -2 at >2 years of age or an identified genetic mutation associated with absence of catch up growth. Seven patients were recruited on the basis of a height -2 SD at >2 years of age with the remaining child recruited at 1.8 years of age displaying no evidence of catch up growth and having a *CUL7* mutation which is associated with absence of postnatal catch up. All of our patients therefore had pathological growth impairment demonstrated by genetic mutations associated with growth failure (n=5), evidence on intrauterine growth restriction on antenatal ultrasound (n=5) and postnatal growth impairment (n=8). Skin fibroblast cell lines were derived from three SGA patients with no defined aetiology, one patient with Russell Silver Syndrome (1p15 hypomethylation), four 3-M syndrome patients and three control subjects. Including those with a defined as well as undefined aetiology allowed us to assess whether their metabolome overall gives any indication of general growth and metabolic disorders in childhood. Biopsies were obtained from the forearm after application of EMLA cream (AstraZeneca, Macclesfield, UK). The 3-M patients included one male with a homozygous *CUL7* mutation (c.4191delC p.H1379HfsX11), one male and one female (siblings) with a homozygous *OBSL1* mutation (c.1273insA, p.T425NfsX40), and one female with a homozygous *CCDC8* mutation (c.84dup, p.L29X). All children had exhibited significant failure of post-natal growth (see Table 3). The three control fibroblast cell lines (two male aged 4 and 9, one female aged 7) were derived from skin obtained during removal

of skin tags from healthy normal statured children and was provided by the University of Manchester Centre for Genomic Medicine. All patients and control subjects were prepubertal at the time the skin samples were obtained.

Informed consent was obtained from parents and the study was approved by the Central Manchester Research Ethics Committee (07/Q1402/67 and 08/H1008/39) (North West Centre for Research Ethics Committees, Manchester, UK).

Cell Culture

Fibroblast cells were cultured in Dulbecco's Modified Eagles Medium (DMEM) (Invitrogen, Paisley, UK) supplemented to a final concentration with 10% fetal bovine serum (Invitrogen, Paisley, UK), 50 units/mL penicillin, 50 μ g/mL streptomycin, 2mM glutamine and 2.5 μ g/mL amphotericin B (Invitrogen, Paisley, UK). Confluent cells passage eight were switched to serum free media 24 hours prior to sampling for metabolomics analysis.

Metabolic footprint collection and preparation

Culture medium (defined as the metabolic footprint) was removed by aspiration and immediately stored at -80°C . Samples were prepared for analysis by lyophilising 200 μ l aliquots (HETO VR MAXI vacuum centrifuge attached to a HETO CT/DW 60E cooling trap; Thermo Life Sciences, Basingstoke, UK).

Metabolic Fingerprint Collection and Preparation

Immediately following the removal of the metabolic footprint sample the cells were rapidly washed twice with 5mL ice cold phosphate buffered saline to remove media contaminants. A quenching solution (80% methanol in water, -40°C) was immediately added to the cells to suppress metabolism. The cells were released by scraping and the resulting suspension was subjected to three freeze/thaw cycles, using liquid nitrogen, to disrupt cell membranes and release the intracellular metabolome to the solution (defined as the metabolic fingerprint). The extraction solution was separated from the cellular biomass by centrifugation (2500g for 5 minutes). Aliquots (1.5 mL) were lyophilised then stored at -80°C prior to further analysis.

Gas Chromatography-Mass Spectrometry

Lyophilised samples (a total of 66 footprint samples and 66 fingerprint samples) were chemically derivatised by addition of an O-methylhydroxylamine solution (50 μ L, 20mg.mL $^{-1}$ in pyridine 60°C for 30 min) (Sigma-Aldrich, Gillingham, UK); followed by addition of 50 μ L MSTFA (N-acetyl-N-(trimethylsilyl)-trifluoroacetamide) (Sigma-Aldrich, Gillingham, UK) and heating at 60°C for 30 min. 20 μ L of a retention index (RI) solution (0.6 mg mL $^{-1}$ C₁₀, C₁₂, C₁₅, C₁₉ and C₂₂ n-alkanes) was added to the derivatised solution. Particulate matter was removed by centrifugation (15 min, 13,3639g) followed by transfer of the supernatant to 300 μ l glass inserts placed in 2mL chromatography vials which were sealed with a PTFE/rubber septum containing screw cap.

Derivatised samples were analysed on a 6890 gas chromatograph and 7890 autosampler (Agilent Technologies, Cheshire, UK) coupled to a Pegasus III electron impact mass spectrometer (Leco, Stockport, UK) as previously described³².

Raw data files (.peg format) acquired from the GC–ToF–MS platform were directly processed by applying the ChromaTof software (Leco Corp. v2.25) as previously described³³. Data for each sample set (metabolic fingerprint and metabolic footprint) were integrated as a single dataset in .xls format for further data processing and analysis. Median values were calculated for data acquired for six technical replicates related to a single subject. All data were normalised to the total peak area ([peak area-metabolite/total peak area-all metabolites]*100). Metabolites were identified by comparison of retention index (RI) and electron impact-derived fragmentation mass spectrum to an in-house mass spectral library³⁴ or by comparison of the mass spectrum to the Golm Metabolome Database (GMD)³⁵ or NIST08 mass spectral library (<http://www.nist.gov/srd/nist1a.cfm>). Four different levels of reporting metabolite annotation or identification are available, as defined by The Metabolomics Standards Initiative (<http://msi-workgroups.sourceforge.net>)³⁶. Level 1 identification was achieved if matching of RI and mass spectrum to a metabolite in the in-house library was achieved. Level 2 identification was achieved by matching to a metabolite present in GMD or NIST08 libraries by mass spectrum only.

Statistical Analysis

Univariate statistical analysis was performed, using the non-parametric Mann Whitney U-test to determine those metabolites showing a statistically significant difference (p-value <0.05) between classes under observation.

Analysis of Associated Biological Function

Metabolic pathway enrichment analysis was performed using the MetaboAnalyst software³⁷. All metabolites identified as statistically significant in metabolic footprint or metabolic fingerprint data were included. The Homo sapiens pathway was applied as well as the hypergeometric test (for over-representation analysis) and relative-betweenness centrality (for pathway topology analysis).

Network analysis of metabolomic data was performed to associate differences in metabolites between SGA and normal cells with all known metabolite and protein interactions and hence assess functional relevance. The Pubchem identifier (<http://pubchem.ncbi.nlm.nih.gov/>) of associated metabolites was mapped to its corresponding object in Ingenuity's Knowledge Base (Qiagen, Redwood City, CA). These molecules, called Network Eligible molecules, were overlaid onto a global molecular network developed from information contained in Ingenuity's Knowledge Base. Interaction Networks were then generated based on the function of these molecules using the Ingenuity Pathways Analysis (IPA) software algorithm. Network data was exported from IPA into Cytoscape 3.2.1 with edge bundling.

Phospho-kinase Array

Cells were serum starved for 24 hours then treated with or without IGF-I (100 ng/mL) (R&D Systems, Abingdon, UK) for 15 minutes. Lysates (a pool of four independent experiments)

were applied to a human phospho MAPK array (R&D systems, Abingdon, UK) in accordance with the manufacturer's protocol. Densitometry was assessed with imageJ (<http://rsb.info.nih.gov/ij/index.html>). Three control cell lines and three SGA cell lines were examined (not including RSS or 3-M syndrome).

Supplementary Material

Refer to Web version on PubMed Central for supplementary material.

Acknowledgments

Financial Support - WBD wishes to thank BBSRC for financial support of The Manchester Centre for Integrative Systems Biology (BBC0082191). IB was supported by an unrestricted educational grant from NovoNordisk. PGM was supported by a Medical Research Clinical Research Training Fellowship (G0700541).

References

1. Births in England and Wales by Characteristics of Birth 2, 2013. Office for National Statistics; 2013.
2. Ananth CV, Vintzileos AM. Distinguishing pathological from constitutional small for gestational age births in population-based studies. *Early human development*. 2009; 85:653–8. [PubMed: 19786331]
3. Wollmann HA. Intrauterine growth restriction: definition and etiology. *Hormone research*. 1998; 49(Suppl 2):1–6.
4. Clayton PE, Cianfarani S, Czernichow P, Johannsson G, Rapaport R, Rogol A. Management of the child born small for gestational age through to adulthood: a consensus statement of the International Societies of Pediatric Endocrinology and the Growth Hormone Research Society. *The Journal of clinical endocrinology and metabolism*. 2007; 92:804–10. [PubMed: 17200164]
5. Saenger P, Czernichow P, Hughes I, Reiter EO. Small for gestational age: short stature and beyond. *Endocrine reviews*. 2007; 28:219–51. [PubMed: 17322454]
6. Klingseisen A, Jackson AP. Mechanisms and pathways of growth failure in primordial dwarfism. *Genes & development*. 2011; 25:2011–24. [PubMed: 21979914]
7. Dunn WB, Broadhurst DI, Atherton HJ, Goodacre R, Griffin JL. Systems level studies of mammalian metabolomes: the roles of mass spectrometry and nuclear magnetic resonance spectroscopy. *Chemical Society reviews*. 2011; 40:387–426. [PubMed: 20717559]
8. Dunn WB, Goodacre R, Neyses L, Mamas M. Integration of metabolomics in heart disease and diabetes research: current achievements and future outlook. *Bioanalysis*. 2011; 3:2205–22. [PubMed: 21985415]
9. Issaq HJ, Fox SD, Chan KC, Veenstra TD. Global proteomics and metabolomics in cancer biomarker discovery. *J Sep Sci*. 2011; 34:3484–92. [PubMed: 22102289]
10. Kenny LC, Broadhurst DI, Dunn W, et al. Robust early pregnancy prediction of later preeclampsia using metabolomic biomarkers. *Hypertension*. 2010; 56:741–9. [PubMed: 20837882]
11. Weiss RH, Kim K. Metabolomics in the study of kidney diseases. *Nat Rev Nephrol*. 2011
12. Mikami T, Aoki M, Kimura T. The application of mass spectrometry to proteomics and metabolomics in biomarker discovery and drug development. *Curr Mol Pharmacol*. 2011
13. Dunn WB, Brown M, Worton SA, et al. Changes in the metabolic footprint of placental explant-conditioned culture medium identifies metabolic disturbances related to hypoxia and pre-eclampsia. *Placenta*. 2009; 30:974–80. [PubMed: 19775752]
14. Boslem E, MacIntosh G, Preston AM, et al. A lipidomic screen of palmitate-treated MIN6 beta-cells links sphingolipid metabolites with endoplasmic reticulum (ER) stress and impaired protein trafficking. *The Biochemical journal*. 2011; 435:267–76. [PubMed: 21265737]
15. Freeth JS, Ayling RM, Whatmore AJ, et al. Human skin fibroblasts as a model of growth hormone (GH) action in GH receptor-positive Laron's syndrome. *Endocrinology*. 1997; 138:55–61. [PubMed: 8977385]

16. Freeth JS, Silva CM, Whatmore AJ, Clayton PE. Activation of the signal transducers and activators of transcription signaling pathway by growth hormone (GH) in skin fibroblasts from normal and GH binding protein-positive Laron Syndrome children. *Endocrinology*. 1998; 139:20–8. [PubMed: 9421393]
17. Silva CM, Kloth MT, Whatmore AJ, et al. GH and epidermal growth factor signaling in normal and Laron syndrome fibroblasts. *Endocrinology*. 2002; 143:2610–7. [PubMed: 12072393]
18. Barker DJ. Adult consequences of fetal growth restriction. *Clinical obstetrics and gynecology*. 2006; 49:270–83. [PubMed: 16721106]
19. Dessi A, Atzori L, Noto A, et al. Metabolomics in newborns with intrauterine growth retardation (IUGR): urine reveals markers of metabolic syndrome. *J Matern Fetal Neonatal Med*. 2011; 24(Suppl 2):35–9. [PubMed: 21767100]
20. Dessi A, Marincola FC, Pattumelli MG, et al. Investigation of the (1)H-NMR based urine metabolomic profiles of IUGR, LGA and AGA newborns on the first day of life. *J Matern Fetal Neonatal Med*. 2014; 27(Suppl 2):13–9. [PubMed: 25284172]
21. Stevens A, Bonshek C, Whatmore A, et al. Insights into the pathophysiology of catch-up compared with non-catch-up growth in children born small for gestational age: an integrated analysis of metabolic and transcriptomic data. *Pharmacogenomics J*. 2014; 14:376–84. [PubMed: 24614687]
22. Horgan RP, Broadhurst DI, Dunn WB, et al. Changes in the metabolic footprint of placental explant-conditioned medium cultured in different oxygen tensions from placentas of small for gestational age and normal pregnancies. *Placenta*. 2010; 31:893–901. [PubMed: 20708797]
23. He Q, Ren P, Kong X, et al. Intrauterine growth restriction alters the metabolome of the serum and jejunum in piglets. *Mol Biosyst*. 2011; 7:2147–55. [PubMed: 21584308]
24. Barberini L, Noto A, Fattuoni C, et al. Urinary metabolomics (GC-MS) reveals that low and high birth weight infants share elevated inositol concentrations at birth. *J Matern Fetal Neonatal Med*. 2014; 27(Suppl 2):20–6. [PubMed: 25284173]
25. Favretto D, Cosmi E, Ragazzi E, et al. Cord blood metabolomic profiling in intrauterine growth restriction. *Analytical and bioanalytical chemistry*. 2012; 402:1109–21. [PubMed: 22101423]
26. Newgard CB, An J, Bain JR, et al. A branched-chain amino acid-related metabolic signature that differentiates obese and lean humans and contributes to insulin resistance. *Cell metabolism*. 2009; 9:311–26. [PubMed: 19356713]
27. Yap IK, Brown IJ, Chan Q, et al. Metabolome-wide association study identifies multiple biomarkers that discriminate north and south Chinese populations at differing risks of cardiovascular disease: INTERMAP study. *Journal of proteome research*. 2010; 9:6647–54. [PubMed: 20853909]
28. Tea I, Le Gall G, Kuster A, et al. 1H-NMR-based metabolic profiling of maternal and umbilical cord blood indicates altered materno-foetal nutrient exchange in preterm infants. *PloS one*. 2012; 7:e29947. [PubMed: 22291897]
29. Rauen KA. The RASopathies. *Annual review of genomics and human genetics*. 2013; 14:355–69.
30. Falik Zaccari TC, Kalfon L, Klar A, et al. Two novel mutations identified in familial cases with Donohue syndrome. *Molecular genetics & genomic medicine*. 2014; 2:64–72. [PubMed: 24498630]
31. Horgan RP, Broadhurst DI, Walsh SK, et al. Metabolic profiling uncovers a phenotypic signature of small for gestational age in early pregnancy. *Journal of proteome research*. 2011; 10:3660–73. [PubMed: 21671558]
32. O'Hagan S, Dunn WB, Brown M, Knowles JD, Kell DB. Closed-loop, multiobjective optimization of analytical instrumentation: gas chromatography/time-of-flight mass spectrometry of the metabolomes of human serum and of yeast fermentations. *Anal Chem*. 2005; 77:290–303. [PubMed: 15623308]
33. Begley P, Francis-McIntyre S, Dunn WB, et al. Development and performance of a gas chromatography-time-of-flight mass spectrometry analysis for large-scale nontargeted metabolomic studies of human serum. *Anal Chem*. 2009; 81:7038–46. [PubMed: 19606840]
34. Brown M, Dunn WB, Dobson P, et al. Mass spectrometry tools and metabolite-specific databases for molecular identification in metabolomics. *Analyst*. 2009; 134:1322–32. [PubMed: 19562197]

35. Kopka J, Schauer N, Krueger S, et al. GMD@CSB.DB: the Golm Metabolome Database. *Bioinformatics*. 2005; 21:1635–8. [PubMed: 15613389]
36. Sumner LW, Amberg A, Barrett D, et al. Proposed minimum reporting standards for chemical analysis. *Metabolomics*. 2007; 3:211–21. [PubMed: 24039616]
37. Xia J, Mandal R, Sinelnikov IV, Broadhurst D, Wishart DS. MetaboAnalyst 2.0--a comprehensive server for metabolomic data analysis. *Nucleic acids research*. 2012; 40:W127–33. [PubMed: 22553367]

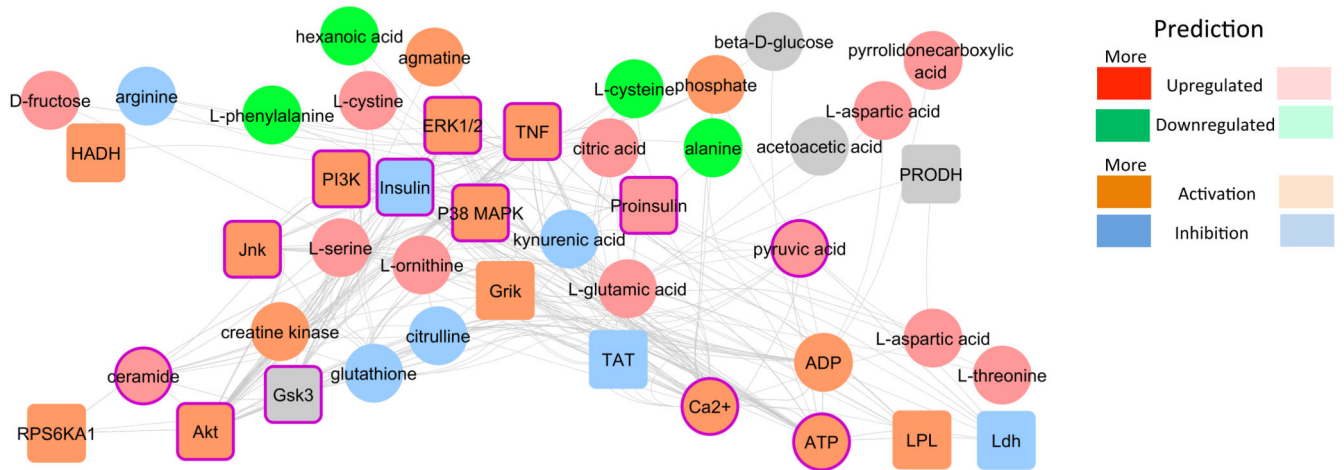


Figure 1. Interaction network of differences in metabolite regulation between control and SGA patient cell lines

Nineteen metabolites were identified as differentially regulated between control and patient cells; these were used to define a network with inferred protein and metabolite interactions (Ingenuity Pathway Analysis Software [IPA]). Predicted activity in the network was calculated by derivation from the findings within the Ingenuity Knowledge Base (IKB) database between the unknown molecule and its known neighbours (Molecule Activity Predictor [MAP] in IPA). Purple highlight indicates involvement with insulin signalling (13/44).

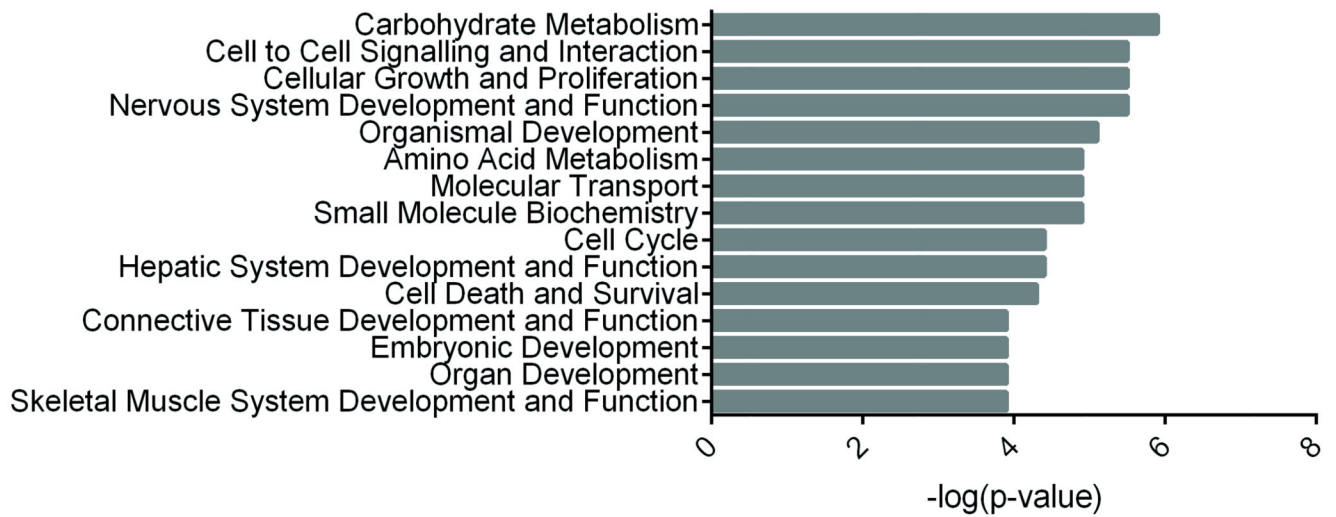


Figure 2. Biological functions associated with differences in metabolite regulation between control and SGA patient cell lines

Biological functions ranked by p-value of Fisher's exact test (negative log).

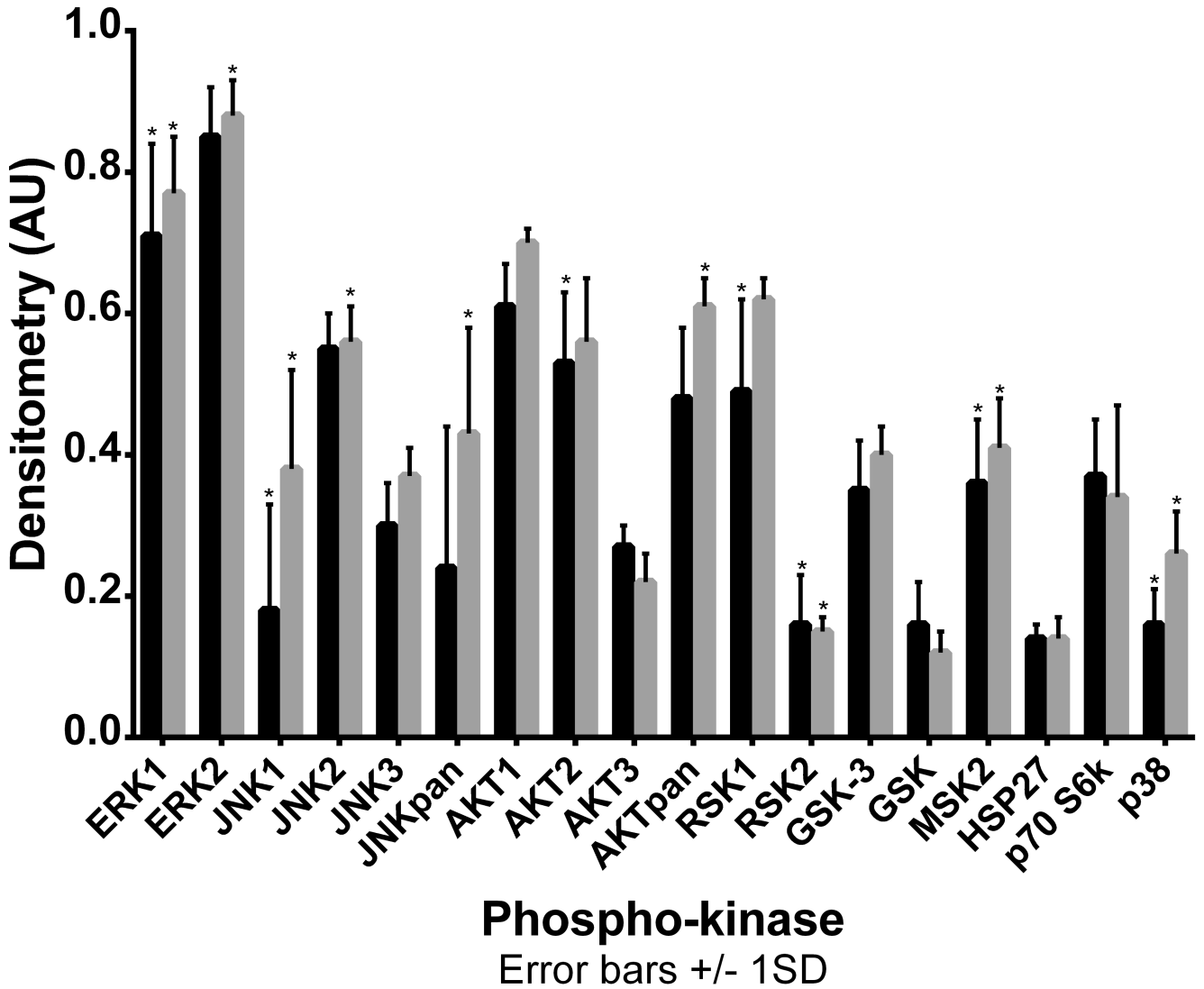


Figure 3. Phospho-kinase activation after stimulation with IGF-I in control and SGA patient cells

In control but not SGA cells IGF-I preferentially activates ERK2 and JNK2 while in SGA but not control cells RSK2 is activated. * $p > 0.05$ for difference between the IGF-I stimulated phospho-kinase activation (shown on graph) and baseline phospho-kinase activity (not shown). Black bars = SGA, Grey bars = Control.

Table 1

Metabolites up- or down-regulated comparing the metabolic fingerprint and metabolic footprint from SGA fibroblasts (n=8) to control cells (n=3). The fold change is calculated as median-SGA/median-control.

Metabolite	Ratio	p-value	Source
Alanine	0.33	0.014	Fingerprint
Threonine	1.25	0.041	Fingerprint
Glutamic acid	1.39	0.025	Fingerprint
Ornithine	1.44	0.014	Fingerprint
Citric acid	1.53	0.041	Fingerprint
Serine	1.65	0.014	Fingerprint
Fructose	1.8	0.014	Fingerprint
Aspartic acid	5.21	0.014	Fingerprint
Alanine	0.19	0.014	Footprint
Cysteine	0.32	0.014	Footprint
2-methyl-3-hydroxybutanoic acid	0.53	0.049	Footprint
3-methylpentanoic acid	0.54	0.014	Footprint
Hexanoic acid	0.58	0.041	Footprint
Phenylalaline	0.65	0.025	Footprint
Aminomalonic acid	0.71	0.041	Footprint
Trimethylamine-N-oxide	1.18	0.025	Footprint
Phosphate	1.26	0.041	Footprint
Pyruvic acid	1.42	0.025	Footprint
Cystine	1.66	0.025	Footprint

Table 2

Metabolic pathways enrichment analysis using the metabolic fingerprint and metabolic footprint metabolites identified as significantly up-/down-regulated between control and SGA cells.

Pathway name	Number of metabolites statistically significant	FDR (q-value)	Metabolites
Cyanoamino acid metabolism	3	0.0074	glycine, serine, alanine
Glycine, serine and threonine metabolism	4	0.0093	threonine, glycine, serine, pyruvate
Alanine, aspartate and glutamate metabolism	3	0.0129	glutamine, aspartate, pyruvate
Methane metabolism	3	0.0291	trimethylamine-N-oxide, glycine, serine
Nitrogen metabolism	3	0.0362	phenylalanine, glutamine, glycine

Table 3

Age, Gender, Height SDS and aetiology of growth impairment

Patient No	Age at presentation (years)	Gender	Birthweight (g)	Gestational Age at Birth (weeks)	Mode of Delivery	Age at Biopsy (years)	Height SDS at time of biopsy	Weight SDS at time of biopsy	Height Velocity SDS at time of biopsy	Evidence of IUGR on antenatal ultrasound	Molecular Aetiology of Growth Impairment
1	6.4	F	640	27	C-section	5.0	-4.5	-6.0	-0.43	No evidence of IUGR recorded but maternal pre-eclampsia.	Unidentified
2	4.7	M	1880	38	C-section	4.8	-2.5	-4.4	-1.0	Yes	Unidentified
3	4.5	F	1077	34	C-section	4.7	-2.3	-3.5	-3.5	Yes – twin to twin transfusion syndrome with death of other twin in utero	Unidentified
4	0.7	M	1757	36	C-section	4.4	-3.3	-2.2	-0.3	Yes with small placenta	Russell Silver Syndrome - 1p15 hypomethylation
5	1.7	M	2140	38	Spontaneous Vaginal	1.8	-5.8	-4.3	-0.7	Yes	CUL7 c.4191delC p.H1379HisX11
6	2.8	F	2380	40	Spontaneous Vaginal	7.9	-3.5	-3.5	-2.0	No	OBSL1 c.1273insA, p.T425NfsX40
7	3.2	M	1927	37	Spontaneous Vaginal	10.3	-4.9	-5.2	-2.1	No	OBSL1 c.1273insA, p.T425NfsX40
8	4.1	F	2409	38	C-section	5.8	-3.3	-4.6	-2.1	Yes	CCDC8 c.84dup, p.L29X